JACS
JOURNAL OF THE AMERICAN CHEMICAL SOCIETY

ARTICLE

pubs.acs.org/JACS

Tetrahedral Atom Ordering in a Zeolite Framework: A Key Factor Affecting Its Physicochemical Properties

Jiho Shin,[†] Deu S. Bhange,[†] Miguel A. Camblor,[‡] Yongjae Lee,[§] Wha Jung Kim,[⊥] In-Sik Nam,[†] and Suk Bong Hong*[,†]

[†]School of Environmental Science and Engineering and Department of Chemical Engineering, POSTECH, Pohang 790-784, Korea

[‡]Instituto de Ciencia de Materiales de Madrid ICMM-CSIC, Consejo Superior de Investigaciones Científicas, c/Sor Juana Inés de la Cruz, 3, 28049 Madrid, Spain

[§]Department of Earth System Sciences, Yonsei University, Seoul 120-749, Korea

[⊥]Department of Materials Chemistry and Engineering, Konkuk University, Seoul 143-701, Korea

Supporting Information

ABSTRACT: Three gallosilicate natrolites with closely similar chemical composition but differing in the distribution of Si and Ga over crystallographically different tetrahedral sites (T-sites) show striking differences in their cation exchange performance. The ability to exchange Na^+ by the larger alkali metal cations decreases upon increasing the size of the cation, as expected, but also with the degree of T-atom ordering. To seek an insight into this phenomenon, the crystal structures of 11 different zeolites, which show variations in degree of T-atom ordering, nature of countercation, and hydration state, have been refined using synchrotron diffraction data. While the three as-made sodium materials were characterized to have a low, medium, and high degree of ordering, respectively, their pore sizes are close to the size of the bare Na^+ cation and much smaller than that of the larger alkali cations, which are nonetheless exchanged into the materials, each one at a different level. Interestingly, large differences are also manifested when the Na^+ back-exchange is performed on the dehydrated K^+ forms, with crystallographic pore sizes too small even to allow the passage of Na^+. Although the thermodynamic data point to small differences in the enthalpy of the Na^+/K^+ exchange in the three materials, comparison of the "static" crystallographic pore sizes and the diameter of the exchanged cations lead us to conclude that during the exchange process these zeolites undergo significant deformations that dynamically open the pores, allowing cation traffic even for Cs^+ in the case of the most disordered material. In addition to the very large topological flexibility typical of the natrolite framework, we propose as a hypothesis that there is an additional flexibility mechanism that decreases the rigidity of the natrolite chain itself and is dependent on preferential siting of Si or Ga on crystallographically different T-sites.

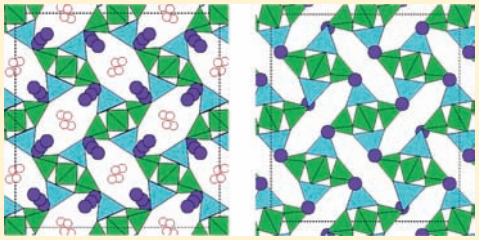

INTRODUCTION

The wide applicability of zeolites in current catalysis, ion exchange, and gas separation and purification technologies relies on the diversity of properties which they can possess, depending primarily on their structure and chemical composition.[1] Zeolites may show varying structure-related properties, such as void volume, accessibility, dimensionality, and shape and size of the pores, and also varying chemistry-related properties, i.e., the nature, number, and strength of catalytically active sites; thermal stability; nature and number of countercations; and hydrophilic/hydrophobic surface properties.[2] Some textural properties, like the micropore surface fraction, may also depend on the zeolite crystal size and/or habit.[3] Up to now, however, only a few studies have demonstrated that the ordered or disordered distribution of tetrahedral atoms (T-atoms) over the crystallographically different T-sites in a given zeolite lattice, i.e., the degree of T-atom ordering, may critically affect the physicochemical properties of this important class of microporous solids with channel and cavity dimensions generally smaller than 20 Å.[4,5]

We previously reported the in situ transformation of a sodium gallosilicate natrolite zeolite (framework type NAT) from an initially crystallized phase showing extensive disorder of Si and Ga over the available T-sites to a final phase with essentially complete order, while its framework topology was preserved.[5] The increased degree of Si−Ga ordering as the crystallization time or temperature increased was demonstrated by ^{29}Si and ^{71}Ga MAS NMR. This was further evidenced by the increased degree of orthorhombic distortion from the ideal tetragonal symmetry, although at that time no detailed structural characterization could be obtained from conventional powder X-ray diffraction data. Most striking was the fact that the chemical composition was essentially unchanged during the transformation, except for a decrease in the water content as the

Received: March 26, 2011
Published: June 02, 2011

Table 1. Characterization Data for Sodium Gallosilicate Natrolite Zeolites with Different Degrees of Si−Ga Ordering

sample ID	T/t,[a] °C/days	unit cell composition[b]	Si/Ga ratio	$\delta_o \times 10^2$[c]	S[d]
Na-GaNAT-I	100/3	$Na_{15.1}Ga_{15.1}Si_{24.9}O_{80}\cdot 19.5H_2O$	1.65	0.373	0.29
Na-GaNAT-II	150/7	$Na_{15.4}Ga_{15.4}Si_{27.0}O_{80}\cdot 17.3H_2O$	1.60	1.552	0.55
Na-GaNAT-III	200/14	$Na_{15.4}Ga_{15.4}Si_{27.0}O_{80}\cdot 16.0H_2O$	1.60	2.697	0.97

[a] Crystallization was performed under slow rotation (60 rpm). [b] Determined from a combination of elemental and thermal analyses based on an orthorhombic unit cell with 40 T atoms. [c] Degree of orthorhombic distortion defined as $(b - a)/(b \times a)^{0.5}$, using the unit cell parameters b and a obtained from the orthorhombic indexing.[5] [d] Long-range order parameter (ref 12) calculated from the crystallographic data on Ga and Si occupancies of T-sites (see the text).

degree of T-atom ordering increased. Furthermore, the transformation proceeded without changes in yield and without phase segregation: the intermediate materials appeared as pure phases with intermediate degrees of ordering, rather than being physical mixtures of the disorder/order end members. Consequently, this transformation affords a continuous series of materials, where the degree of Si−Ga ordering can be controlled at will by properly selecting the crystallization time or temperature. According to periodic ab initio calculations on the energetics of Ga and Si sitings over crystallographically different T-sites and considering also the cost of Ga−O−Ga pairings (i.e., violations of the extended Loewenstein's rule),[6] we were able to conclude that the transformation was driven by preferential siting of Si on the lower multiplicity T-site, i.e., the T-site involved in less 4-rings, and by Loewenstein's rule: in the NAT topology with a Si/Ga ratio of 1.5, preferential siting of Si on the lower multiplicity site forces Ga into the high multiplicity site and, in order to minimize the cost of anti-Loewenstenian pairings, this site has to split into two nonequivalent sites occupied by Ga and Si, respectively. Full T-atom ordering is thus imposed.

These findings are, in our opinion, an outstanding opportunity to investigate in detail how T-atom ordering can influence the physicochemical properties of a zeolite. In fact, we have already observed significant differences along the disorder−order series, in addition to those easily and directly explained by different degrees of ordering on the basis of ^{29}Si and ^{71}Ga MAS NMR results.[5] For example, as commented above, while the cell volume remained fairly constant (within 1%), a significant decrease in water content (exceeding a 20% decrease), with an increase in the temperature needed for water desorption (up to around 40 °C), was observed as T-atom ordering increased. Here we have prepared three sodium gallosilicate natrolites with fairly close chemical composition but different degrees of T-atom ordering and have investigated how ordering determines the cation exchange ability of these materials. Detailed structural characterization results of as-made Na^+ and cation-exchanged materials in hydrated and, when stable, their dehydrated form are also provided. The ensuing discussion lead us to propose the hypothesis that, in addition to thermodynamic effects, T-atom ordering in the NAT family of zeolites might determine the overall flexibility of the framework and, hence, the cation exchange properties of the materials.

EXPERIMENTAL SECTION

Synthesis. Three sodium gallosilicate natrolites with similar Si/Ga ratios but different degrees of Si−Ga ordering were synthesized using the same synthesis mixture ($6.0Na_2O\cdot 1.0Ga_2O_3\cdot 10SiO_2\cdot 150H_2O$) under the conditions described elsewhere[5,7] and summarized in Table 1. Here we refer to these three samples as Na-GaNAT-I, Na-GaNAT-II, and Na-GaNAT-III, respectively. Various cation forms of natrolite zeolites prepared here were obtained by exchanging twice their as-made Na^+ form with 1.0 M aqueous nitrate solutions of Li^+, K^+, Rb^+, Cs^+, Ca^{2+}, and La^{3+} ions at 0.02 g mL^{-1} and 60 °C for 4 h. Also, Na^+ back-exchange was carried out in a similar manner. For detailed structural analysis, the samples were exchanged four times under the conditions described above, to maximize the degree of cation exchange. The finally exchanged samples, as well as their as-made ones, were dried overnight at room temperature. If required, the samples were dehydrated by calcining at 500 °C for 4 h. The as-made, ion-exchanged, calcined, and Na^+ back-exchanged samples were designated by attaching the suffixes A, E, C, and B in parentheses to their names, respectively. For example, NaK-GaNAT-I(ECB) indicates that the as-made GaNAT material with a low degree of T-atom ordering (see below) was exchanged with K^+, calcined at 500 °C for 4 h, and then back-exchanged with Na^+.

Characterization. Powder X-ray diffraction (XRD) patterns were recorded on a PANalytical XPert diffractometer (Cu Kα radiation) with an XCelerator detector. Data were collected with a fixed divergence slit (0.50°) and Soller slits (incident and diffracted = 0.04 rad). In situ high-temperature XRD experiments were performed in Bragg−Brentano geometry using the same diffractometer equipped with an Edmund Bühler HDK 1.4 high-temperature attachment. Elemental analysis for Si and Ga was carried out by a Jarrell-Ash Polyscan 61E inductively coupled plasma (ICP) spectrometer in combination with a Perkin-Elmer 5000 atomic absorption spectrophotometer. The Li^+, Na^+, K^+, and Ca^{2+} contents of the samples were determined by a Thermo Elemental ICAP 6500 ICP-AES spectrometer, while the Rb^+, Cs^+, and La^{3+} contents were done by a Thermo Elemental X series ICP-MS spectrometer. Thermogravimetric and differential thermal analyses (TGA/DTA) were performed on an SII EXSTAR 6000 thermal analyzer at a heating rate of 10 °C min^{-1}. All samples were exposed to ambient air at least for 3 days prior to thermal analysis. When rehydration proved difficult (see below), in addition, the zeolite powder was immersed into water and dried in the manner given above. The He and H_2 sorption isotherms were measured using a Mirae SI nanoPorosity-XG analyzer. ^{29}Si MAS NMR measurements were carried out on a Varian Inova 300 spectrometer at a spinning rate of 6.0 kHz. The spectra were recorded at a ^{29}Si frequency of 59.590 MHz with a $\pi/2$ rad pulse length of 5.0 μs, recycle delays of 30−120 s, and an acquisition of about 5000 pulse transients. The ^{29}Si chemical shifts are reported relative to TMS. All spectral deconvolution and simulation were performed using the PeakFit curve-fitting program.

Structural Analysis. Synchrotron diffraction data for all gallosilicate natrolites prepared in this study were collected on the 8C2 beamline equipped with a ceramic furnace of the Pohang Acceleration Laboratory (Pohang, Korea) using monochromated X-rays (λ = 1.5490 or 1.5495 Å). The detector arm of the vertical scan diffractometer consists of seven sets of Soller slits, flat Ge(111) crystal analyzers, antiscatter baffles, and scintillation detectors, with each set separated by 20°. Data were obtained on the sample at room temperature in flat plate mode, with a step size of 0.01° and overlaps of 2° to the next detector bank over the 2θ range 10°−131°. The framework structure and the position of

extraframework cations were determined by direct methods using the program EXPO2009.[8] The structure obtained in this way was further refined via the Rietveld method using the GSAS suite of programs and EXPGUI graphical interface,[9] with soft restraints applied to T−O and O−O distances in the tetrahedral framework (1.70 and 2.80 Å, respectively). Peak shape was modeled using the pseudo-Voigt profile function.[10] The simultaneous refinement of the Ga and Si fraction (Ga + Si = 1.0) in all T-sites, with the total Ga content of the sample constrained to the value suggested by elemental analysis, was carried out in the later stage of refinements of corresponding as-made forms. The bond restraint distances mentioned above were adopted as per the final refinement results of fractional occupancies of Si and Ga. The refined occupancies of T-sites in as-made Na−GaNAT materials were fixed during the refinements of their corresponding cation exchanged hydrated and dehydrated forms. The extraframework cations and water molecules were located along the elliptical channels from difference Fourier syntheses. The convergence was achieved by refining simultaneously all profile parameters; scale factor; lattice constants; 2θ zero-point, atomic positional, and thermal displacement parameters; and occupancy factors for the framework atoms, extraframework cations, and water O atoms.

RESULTS

Variations in T-Atom Ordering. We have synthesized three gallosilicate natrolites in sodium form under different conditions of crystallization temperature and time, as given in Table 1, which also lists their chemical compositions. The Ga and Na contents are closely similar in the three materials, but significant differences are found in their water content. The structural characterization of these materials reveals large differences in the distribution of Si and Ga among crystallographically different T-sites (see below), although all the three belong to the NAT zeolite framework type.[11] The powder XRD patterns recorded with a conventional laboratory powder diffractometer could be indexed as tetragonal ($I\bar{4}2d$, Na-GaNAT-I), or orthorhombic (*Fdd*2, Na-GaNAT-II and GaNAT-III). However, the synchrotron diffraction data of Na-GaNAT-I could be better indexed as orthorhombic, space group *Fdd*2. As listed in Table 1, on the other hand, the three materials show different degrees of orthorhombic distortion (δ_o; see Table 1) from the ideal tetragonal cell that increase as the crystallization conditions harshen (i.e., as crystallization time and temperature increased). All these results perfectly fit into our already reported description of this system, which shows an in situ disorder−order transformation characterized by an increase in the degree of Si−Ga ordering over the available T-sites, while the NAT topology is preserved and the chemical composition is essentially constant (except for the water content).[5,7]

Table 1 also contains information on T-atom ordering through the long-range order parameter *S* proposed by Alberti et al.[12] We derived this parameter from the relative occupancies of different sites by Ga or Si in the structures of the three as-made materials obtained by Rietveld refinements of synchrotron diffraction data. Full structural details and Rietveld plots can be found in Supporting Information Tables S1 and S4 and Figure S1, and the general structural features are discussed below. The parameter *S* is 0 for complete Ga−Si disorder and 1 for full order. The values in our three as-made natrolites i.e., Na-GaNAT-I (0.29), Na-GaNAT-II (0.55), and Na-GaNAT-III (0.97), confirm that they indeed show a low, intermediate, and high degree of Si−Ga ordering, respectively.

Cation Exchange. On the basis of their chemical composition, the maximum theoretical cation exchange capacity, CEC, of the three materials is around 4.1 mmol g^{-1}, with variations smaller than 4% at most. Table 2 summarizes cation exchange results using the three as-made natrolites, where there are two noticeable aspects to highlight.

Table 2. Ion Exchanges in Sodium Gallosilicate Natrolites[a]

ion exchanged	r,[b] Å	degree of exchange,[c] % Na-GaNAT-I	Na-GaNAT-II	Na-GaNAT-III
Li^+	0.59 (4), 0.76 (6)	40	12	1
K^+	1.38 (6), 1.51(8)	99	99	84
Rb^+	1.52 (6), 1.61(8)	99	66	6
Cs^+	1.67 (6), 1.74 (8)	16	<1	<1
Ca^{2+}	1.00 (6), 1.12 (8)	<1	<1	<1
La^{3+}	1.03 (6), 1.16 (8)	<1	<1	<1

[a] All nitrate solutions 1.0 M; 2 g of solid/100 mL of solution; 60 ± 1 °C, 4 h, twice. Each initial solution contains a 180-excess of exchanging Na^+ ion. [b] Effective ionic radius for the most frequent coordination number given in parentheses.[19] For comparison, Na^+ values are 1.02 (6), 1.18 (8). [c] Calculated from the difference between the molar content of exchanged ion and that of remaining Na^+ ion in each zeolite.

First, the divalent Ca^{2+} and trivalent La^{3+} cations are excluded, despite their sizes being smaller than that of K^+, which can be exchanged into the three phases, suggesting a high selectivity to monovalent cations. This contrasts with the high selectivity for divalent and trivalent cations over monovalent cations generally found with high-alumina zeolites.[13] About 60 years ago Barrer already reported that analcime (ANA), as opposed to mordenite (MOR) and chabazite (CHA), also shows a high selectivity toward monovalent cations.[14] On the basis of this finding, he proposed that the lack of divalent cation exchange may sometimes reflect the need to avoid "a state of local disbalance of cationic and anionic charges" that would otherwise occur, if space restrictions in the channel hindered the location of a cation close to two anionic framework charges. Such space restrictions, however, do not clearly exist in natrolites: in fact, a natural calcium aluminosilicate with the NAT topology, scolecite, exists.[15]

Second, and most important within the scope of this work, exchange with monovalent cations (Li^+, K^+, Rb^+, and Cs^+) reveals large differences in the cation exchange ability of the three materials: Na-GaNAT-I is much better a cation exchanger than Na-GaNAT-II, which is in its turn better than Na-GaNAT-III (Table 2). In these experiments, where the cation exchange is done twice, Na^+ in Na-GaNAT-I is completely replaced by K^+ and Rb^+, while partial but still substantial exchange is accomplished with Li^+ and Cs^+. By contrast, Na-GaNAT-III shows a high but incomplete level of K^+ exchange, while a small degree of exchange is realized with Rb^+, and all the other cations are essentially excluded from exchange. The material with an intermediate degree of order shows an intermediate behavior, as Na^+ is completely exchanged by K^+ while significant but incomplete levels of exchange are achieved with Rb^+ and Li^+.

Among the monovalent cations tested, the case of Li^+ is special because typically "all zeolites prefer Na^+ to Li^+".[13] This observation has been rationalized by the high hydration energy of Li^+, although Barrer pointed out that he encountered the same difficulty in exchanging Li^+ into analcime, chabazite, and mordenite in the absence of water, using molten salts.[14] What is true is that Li^+-containing compounds, due to the small size and high polarization power of this cation, generally exhibit a higher degree of covalent bonding than the equivalent compounds of

Table 3. Chemical Compositions of Gallosilicate Natrolites with Different Degree of Si−Ga Ordering after Various Cation Exchange and Calcination Steps

sample ID[a]	unit cell composition[b]	degree of exchange, %
Na-GaNAT-I(A)	$Na_{15.1}Ga_{15.1}Si_{24.9}O_{80}\cdot 19.5H_2O$	–
K-GaNAT-I(E)	$K_{15.1}Ga_{15.1}Si_{24.9}O_{80}\cdot 20.4H_2O$	100
NaK-GaNAT-I(EB)	$Na_{15.1}Ga_{15.1}Si_{24.9}O_{80}\cdot 19.7H_2O$	100
NaK-GaNAT-I(ECB)	$Na_{7.5}K_{7.6}Ga_{15.1}Si_{24.9}O_{80}\cdot 10.5H_2O$	50
Rb-GaNAT-I(E)	$Na_{0.2}Rb_{14.9}Ga_{15.1}Si_{24.9}O_{80}\cdot 20.8H_2O$	99
NaRb-GaNAT-I(EB)	$Na_{13.5}Rb_{1.6}Ga_{15.1}Si_{24.9}O_{80}\cdot 19.1H_2O$	89
NaRb-GaNAT-I(ECB)	$Na_{1.2}Rb_{13.9}Ga_{15.1}Si_{24.9}O_{80}\cdot 2.4H_2O$	7
Na-GaNAT-II(A)	$Na_{15.4}Ga_{15.4}Si_{24.6}O_{80}\cdot 17.3H_2O$	–
K-GaNAT-II(E)	$Na_{0.1}K_{15.3}Ga_{15.4}Si_{24.6}O_{80}\cdot 18.8H_2O$	99
NaK-GaNAT-II(EB)	$Na_{15.4}Ga_{15.4}Si_{24.6}O_{80}\cdot 18.4H_2O$	100
NaK-GaNAT-II(ECB)	$Na_{5.1}K_{10.3}Ga_{15.4}Si_{24.6}O_{80}\cdot 8.0H_2O$	32
Na-GaNAT-III(A)	$Na_{15.4}Ga_{15.4}Si_{24.6}O_{80}\cdot 16.0H_2O$	–
K-GaNAT-III(E)	$Na_{3.2}K_{12.2}Ga_{15.4}Si_{24.6}O_{80}\cdot 16.4H_2O$	79
NaK-GaNAT-III(EB)	$Na_{15.4}Ga_{15.4}Si_{24.6}O_{80}\cdot 16.0H_2O$	100
NaK-GaNAT-III(ECB)	$Na_{3.2}K_{12.2}Ga_{15.4}Si_{24.6}O_{80}\cdot 3.3H_2O$	0

[a] The suffix A, E, C, or B is attached in parentheses to the zeolite name in order to distinguish between the as-made, ion-exchanged, calcined, or Na^+ back-exchanged samples, respectively. [b] Determined from a combination of elemental and thermal analyses by assuming an orthorhombic unit cell with 40 T atoms.

any other alkali cation,[16] explaining why exchange of Li^+ ions into zeolites is unfavorable. For materials with a similar chemical composition, on the other hand, one would expect no large differences in their CEC, unless significant variations in pore size existed. If they present the same zeolite topology, large pore variations are not expected, either. However, taking aside Li^+, the results in Table 2 suggest that for monovalent cations the exchange process in our gallosilicate natrolites is impeded as the size of the cation increases and the degree of Si−Ga ordering in the zeolite increases. To the best of our knowledge, this is the first example ever in which the cation exchange ability of zeolitic materials apparently depends on the degree of T-atom ordering.

To understand this apparent dependency and the different exchange ability of the three materials, we have studied in detail not only the three as-made Na-GaNAT materials but also the ones that can be almost fully exchanged after four successive treatments with 1.0 M KNO_3 or $RbNO_3$ solutions, i.e., K-GaNAT-I, K-GaNAT-II, K-GaNAT-III, and Rb-GaNAT-I materials. The materials were studied in their hydrated and, when stable, dehydrated forms, and their structures will be commented on below. The chemical compositions of the as-made and fully exchanged materials, together with those of the materials after experiments of back-exchange to their original sodium forms, are listed in Table 3. These data reveal no differences between uncalcined potassium materials with varying degrees of T-atom ordering, as all attained a close to complete Na^+ back-exchange. By contrast, only 89% of Rb^+ in the Rb^+-exchanged Na-GaNAT-I sample, i.e., NaRb-GaNAT-I(EB), were exchanged by Na^+ after two cycles of back-exchange. The water content of all the (uncalcined) materials appears to correlate to the degree of ordering, irrespective of the nature of the countercation: it is approximately 20, 18, and 16 H_2O/unit cell (uc) for GaNAT-I, GaNAT-II, and GaNAT-III, respectively.

However, as opposed to the behavior found for uncalcined materials, and very interestingly, when Na^+ back-exchange was performed twice on the calcined potassium gallosilicate natrolites, large differences were observed again, depending on the degree of T-atom ordering (Table 3): the degree of back-exchange is around 50, 32, and 0% for K-GaNAT-I(EC), K-GaNAT-II(EC), and K-GaNAT-III(EC), respectively. Table 3 also shows that calcination at 500 °C led to a significant decrease in water content from 16 to 3 H_2O/uc of this highly ordered K-GaNAT material. Since its structure remains intact after the calcination step (Supporting Information Figure S2), we considered the possibility that the calcined K-GaNAT-III material could not adsorb H_2O with a Lennard-Jones (L-J) size of 2.65 Å, the third smallest molecule.[17]

To further investigate the fully exchanged potassium materials, we have prepared K-GaNAT-II and K-GaNAT-III with a 99% degree of exchange by treating with 1.0 M KNO_3 solutions four times at 60 °C. These samples, plus the K-GaNAT-I directly obtained after two exchanges, were calcined at 500 °C and then back-exchanged four times with Na^+. The TGA/DTA traces in Figure 1 reveal that the weight loss in calcined K-GaNAT samples, due to the desorption of water, notably decreases upon increasing the degree of Si−Ga ordering. Consequently, K-GaNAT-III(EC), i.e., the calcined K-GaNAT-III sample, gives a weight loss smaller than 1 wt % between the room temperature and 800 °C. This is also the case for its immersion in water, demonstrating a notable inability of K-GaNAT-III(EC) to rehydrate. In fact, we found that this material exhibits essentially zero uptake for He and H_2 with L-J sizes of 2.60 and 2.89 Å, respectively, at liquid nitrogen temperature up to 760 Torr partial pressure. Thus, the K-GaNAT-III material can be considered as the first example where a microporous material becomes essentially nonmicroporous via a simple ion exchange followed by calcination, while maintaining its structural integrity. Table 3 also shows that not only Na^+ back-exchange of calcined Rb-GaNAT-I is more difficult than that of calcined K-GaNAT-I with the same degree of ordering, but also the water content of the back-exchanged material is much smaller.

In situ powder XRD experiments show that, unlike their Na counterparts,[7] all the three K^+-exchanged GaNAT materials are thermally stable at temperatures up to at least 800 °C, which affords the preparation of the dehydrated materials. A major difference in the thermal evolution of the Na^+ and K^+ forms of gallosilicate natrolites refers to the dehydration temperature that is much lower for the latter. As seen in Figure 1, dehydration occurs in the 300−400 °C range for Na-GaNAT materials, with the dehydration temperature increasing as the degree of T-atom ordering increases, while the K^+-exchanged materials dehydrate below 150 °C. In our opinion, this low dehydration temperature affords the higher stability of K-GaNAT materials, in a similar way as we already proposed to explain the outstanding thermal stability of PST-1, a synthetic potassium gallosilicate natrolite with a high Ga content (Si/Ga = 1.28): when the temperature is high enough to afford structural modifications by reorganization of T−O−T bonds, there is no water that can mediate such a reorganization.[18]

Structural Details. We have refined the crystal structures of a total of 11 gallosilicate natrolites prepared in this work: the three hydrated Na-GaNAT materials, the three hydrated and three dehydrated K^+-exchanged ones, and the hydrated and dehydrated Rb-GaNAT-I samples. Full details are provided in Supporting Information Tables S1−S9 and Figures S1, S3, and S4. When all

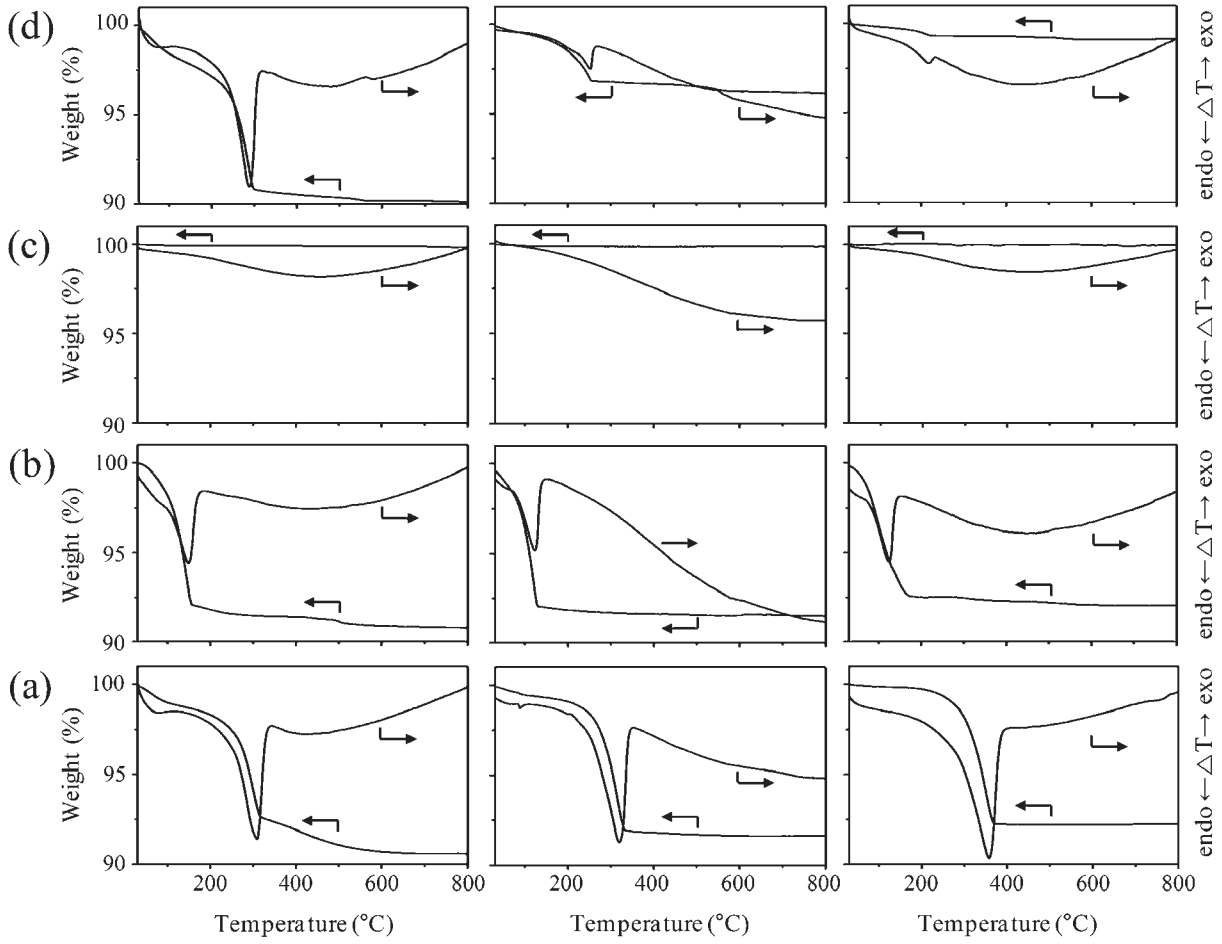

Figure 1. TGA/DTA traces of the (a) as-made Na^+, (b) K^+-exchanged, (c) K^+-exchanged and calcined, and (d) K^+-exchanged, calcined, and then Na^+ back-exchanged forms of GaNAT-I (left), GaNAT-II (middle), and GaNAT-III (right) materials.

the structures are compared, we can see that, with respect to pore size and shape and other structural details (Table 4), the degree of T-atom ordering makes little difference among them, if the countercation and hydration state (hydrated or dehydrated) is maintained. In particular, when the structures of three as-made Na-GaNAT materials are considered, the main 9-ring channels are highly elliptical but quite similar in size and shape to one another (Figure 2). The minimum apertures of their 9-rings are in all cases very small, with O−O distances across the window that are so small that one would expect that cation exchange would require quite forcing conditions: the 9-ring-openings (2.21, 2.22, and 2.12 Å for Na-GaNAT-I(A), Na-GaNAT-II(A), and Na-GaNAT-III(A), respectively) are similar to the diameter of the bare dehydrated Na^+ ion (2.04 Å) and much smaller than the size of bare K^+, Rb^+, and Cs^+ ions (2.76, 3.04, and 3.34 Å, respectively). Throughout this work, the size of the cations used for discussion will be based on the effective ionic radii for the cations in octahedral coordination, as determined by Shannon.[19] It is important to understand that diffusion in natrolite zeolites always implies the 9-rings. While the 9-ring pores are built by stacked 9-rings, in the 8-ring pores consecutive 8-rings are displaced by half a unit cell *c* edge. Thus, after passing an 8-ring, it is necessary to pass a 9-ring before reaching the next 8-ring. As a consequence, if the minimum aperture is smaller in the 9-rings than in the 8-rings, as is frequently the case, then diffusion through all the pores is limited by the minimum aperture of the 9-ring.

Table 4. Important Structural Parameters for 11 Gallosilicate Natrolites with Different Degrees of Si−Ga Ordering, Countercations, and Hydration States

material	Ψ,[a] deg	θ,[a] deg	$d_{O-O(9\text{-ring})}$,[b] Å	$d_{O-O(8\text{-ring})}$,[b] Å
Na-GaNAT-I(A)	24.3	129.8(3)	2.21	2.44
Na-GaNAT-II(A)	24.2	130.3(3)	2.22	2.47
Na-GaNAT-III(A)	25.2	126.6(2)	2.12	2.53
K-GaNAT-I(E)	15.5	141.3(2)	3.25	2.66
K-GaNAT-II(E)	16.6	139.2(4)	3.13	2.65
K-GaNAT-III(E)	18.2	135.6(2)	2.94	2.69
K-GaNAT-I(EC)	30.1	118.3(3)	1.47	2.18
K-GaNAT-II(EC)	29.6	118.7(4)	1.52	2.15
K-GaNAT-III(EC)	30.8	116.6(2)	1.41	2.19
Rb-GaNAT-I(E)	14.7	144.9(2)	3.36	2.73
Rb-GaNAT-I(EC)	28.5	122.0(3)	1.72	2.44

[a] Ψ is the average chain rotation angle of the T_5O_{10} unit, and θ the T−O2−T on which the rotation of chains hinges (see the text). [b] The O−O window distance that is the minimum crystallographic dimension across the 9- or 8-rings, after subtracting the van der Waals radius (2 × 1.35 Å) of both O atoms. Notice that diffusion along the sinusoidal 8-ring pores requires passing also through the 9-rings (see the text).

As shown in Figure 3, on the other hand, all the hydrated potassium materials have larger and more circular pores, with

dx.doi.org/10.1021/ja202739j |*J. Am. Chem. Soc.* 2011, 133, 10587–10598

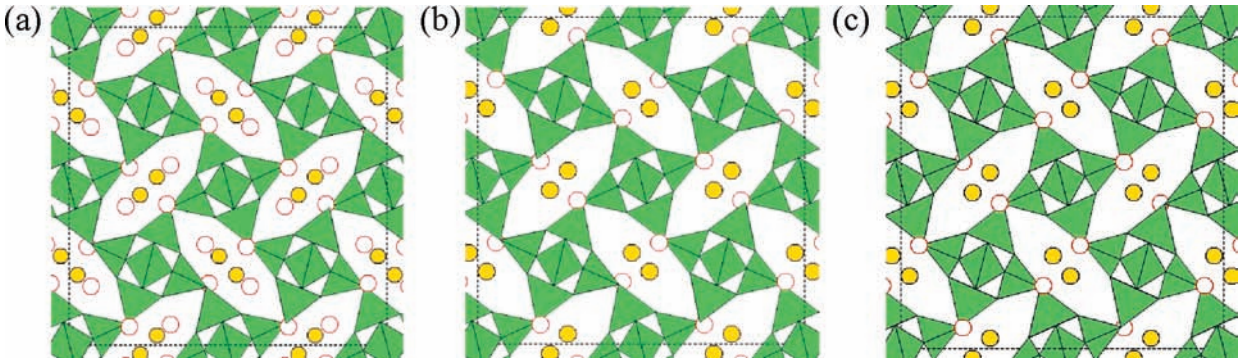

Figure 2. Polyhedral representations of as-made, hydrated (a) Na-GaNAT-I, (b) Na-GaNAT-II, and (c) Na-GaNAT-III zeolites viewed along [001], the chain/channel axis. Filled spheres and open circles represent the Na^+ ions and water O atoms, respectively.

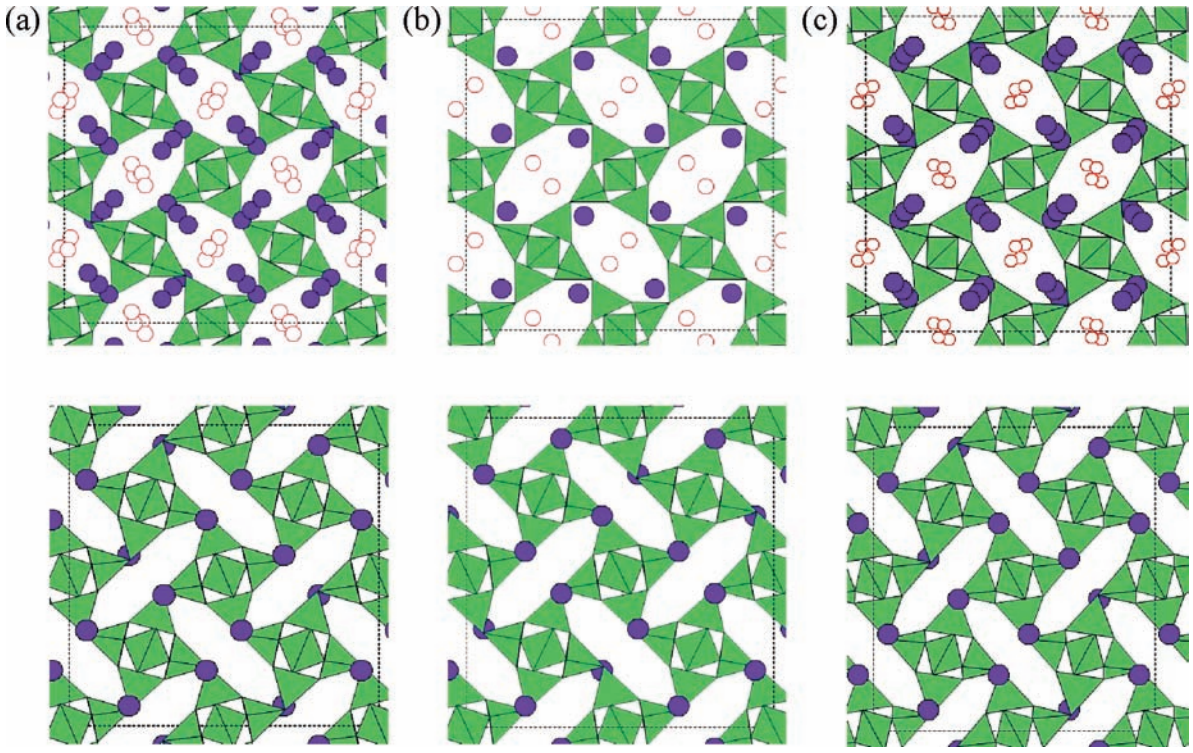

Figure 3. Polyhedral representations of (a) K-GaNAT-I, (b) K-GaNAT-II, and (c) K-GaNAT-III materials hydrated (top) under ambient conditions and dehydrated (bottom) at 500 °C for 4 h viewed along [001], the chain/channel axis. Filled spheres and open circles represent the K^+ ions and water O atoms, respectively.

minimum apertures of 3.25, 3.13, and 2.94 Å for the 9-ring pores in K-GaNAT-I(E), K-GaNAT-II(E), and K-GaNAT-III(E), respectively, always larger than the diameter of K^+. This may explain why they readily back-exchange to the Na^+ form without apparent dependency on the degree of T-atom ordering. After calcination, however, the dehydrated potassium gallosilicate natrolites all present highly elliptical and very small 9-ring pores: 1.47, 1.52, and 1.41 Å for K-GaNAT-I(EC), K-GaNAT-II(EC), and K-GaNAT-III(EC), respectively. Despite this limitation, Na^+ back-exchange is still possible, to some extent, and the degree of ion exchange increases with the degree of T-atom disordering, revealing no correlation to the crystallographic pore sizes. The crystal structures of the hydrated and dehydrated forms of Rb-GaNAT-I in Figure 4 also show differences in the pore size. While the more circular and larger 9-ring pores with minimum aperture of 3.36 Å in Rb-GaNAT-I(E) accounts for the easy back-exchange to the Na^+ form, the dehydration induced closing of the 9- and 8-ring pores to 1.72 and 2.44 Å, respectively, explains the difficulties encountered in the back-exchange to Na^+ form. As a final consideration regarding the structural work, the large flexibility of the NAT topology, repeatedly reported in the literature of aluminosilicate natrolite minerals with a complete degree of Si—Al ordering,[20,21] is also largely apparent for the gallosilicate ones presented here. For example, dehydration of the K^+-exchanged materials bears a 19—20% volume shrinkage (16% for Rb-GaNAT-I). Flexibility issues will be discussed in the next section.

^{29}Si MAS NMR Spectroscopy. During the structural refinements of gallosilicate natrolites prepared here, we have considered that cation exchange and dehydration processes would not

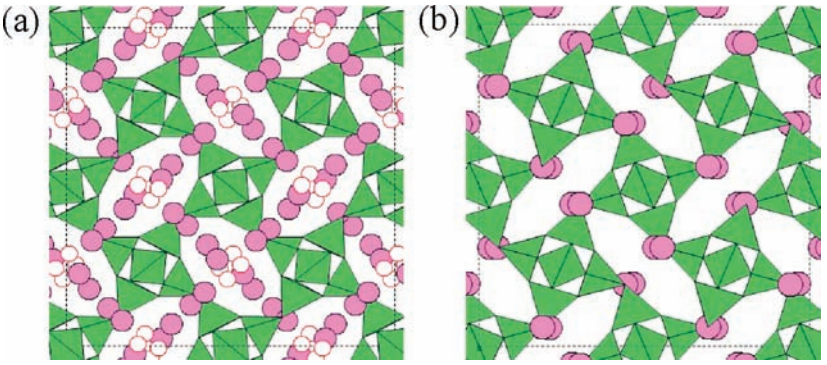

Figure 4. Polyhedral representations of (a) hydrated and (b) dehydrated Rb-GaNAT-I materials viewed along [001], the chain/channel axis. Filled spheres and open circles represent the Rb^+ ions and water O atoms, respectively.

significantly alter the degree of Si−Ga ordering. This is because cation exchange occurs under mild conditions and dehydration of the K^+ and Rb^+ forms occurs essentially in the absence of water, since both dehydrate at very low temperatures (Figure 1 and Supporting Information Figure S5). Thus, the breaking and reorganization of T−O−T angles and the concerted migration of Si and Ga that would be required for altering T-atom ordering must be very limited. To more conclusively check this assumption, we have collected the ^{29}Si MAS NMR spectra of the most ordered and most disordered sodium materials, as well as of the corresponding hydrated and dehydrated K^+ forms and, most importantly, the corresponding materials after the Na^+ back-exchange experiments.

As shown in Figure 5, the ^{29}Si MAS NMR spectrum of Na-GaNAT-III(A) clearly reveals a high degree of T-atom ordering, with mainly two resonances at −94.7 and −84.6 ppm in a 1:2 ratio that can be assigned to Si(2Si,2Ga) and Si(1Si,3Ga), respectively. The observed chemical shifts are within 2 ppm from those calculated using the equation of Cho et al.[7a] and the average T−O−T angles derived from the structural work (Supporting Information Tables S7 and S8). After K^+ ion exchange, in addition, there are still two main resonances, now shifted to lower field, specially the Si(2Si,2Ga) resonance, due to the decreased average T−O−T angle (experimental and calculated chemical shifts still agree very well; see Table 5). This supports that K^+/Na^+ exchange did not affect significantly the degree of ordering. A very large shift to lower field of both resonances caused by calcination points to a large decrease in average T−O−T angles that generally agrees with the crystallographic results, although in this case the disagreement between calculated and experimentally observed chemical shifts is slightly larger (up to 3 ppm). This is not unexpected, because the structural refinement of the dehydrated K-GaNAT-III(EC) material proved more difficult: the final residuals were slightly larger than for the other structures of this series, and the use of soft constrains on T−O and O−O distances may bias the resulting structure to some extent. Nonetheless, the ^{29}Si MAS NMR results are fully consistent with its high degree of T-atom ordering. Finally, since we were not able to back-exchange this dehydrated material to its Na^+ form, the spectrum of the resulting material is much similar to that of K-GaNAT-III(EC), supporting that little back-exchange and limited rehydration occurred.

Figure 5 also shows that the ^{29}Si MAS NMR spectra of GaNAT-I materials are far more complicated and difficult to interpret, because the large degree of Si−Ga disordering over the three crystallographically different T-sites in the refined structures impedes the extraction of the population of Si($(n-1)$Si, nGa) species with $n = 0-4$ over each of the three T-sites and also because of the difficulty in unambiguously deconvoluting the spectra. The spectrum of Na-GaNAT-I(A), however, agrees remarkably well with the expectations: by the naked eye we can distinguish no less than eight heavily overlapped resonances spanning across all the Si($(n-1)$Si,nGa) regions of chemical shifts. In addition, the existence of more than five resonances implies a certain resolution of Si($(n-1)$Si,nGa) resonances in different crystallographic sites. A deconvolution of this spectrum using 10 lines agree well with the refined structure (Table 6): the disagreement between calculated and observed chemical shifts is generally lower than 2 ppm, and the calculated Si/Ga ratio of 1.69 is reasonably close to the ratio found by elemental analysis (1.65).

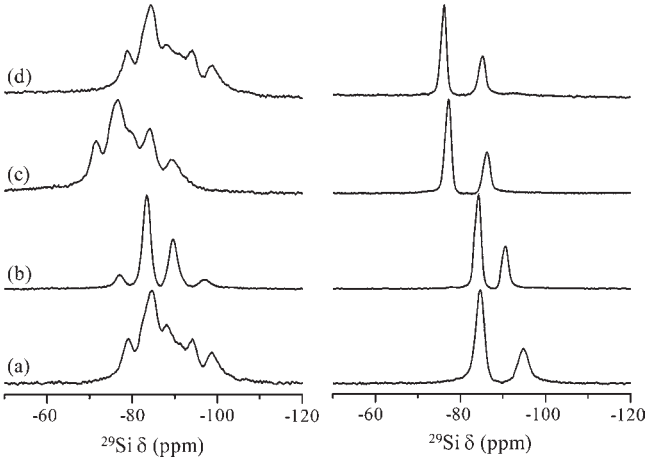

Figure 5. ^{29}Si MAS NMR spectra of the (a) as-made Na^+, (b) K^+-exchanged, (c) K^+-exchanged and calcined, and (d) K^+-exchanged, calcined, and then Na^+ back-exchanged forms of the disordered GaNAT-I (left) and ordered GaNAT-III (right) materials.

By contrast, the ^{29}Si MAS NMR spectrum of the hydrated K-NAT-I(E) material is surprisingly much simpler. Now, there appear to be fewer lines with only a marginal shift to lower field. In the refined structure the average T−O−T angles (133.8°, 134.5°, and 134.9°, for T1, T2, and T3 sites, respectively) are in a narrow range of barely over 1°, while in the parent material the range of average angles was 4° (138.4°, 134.5°, and 134.4°, respectively). This narrower distribution of average T−O−T

dx.doi.org/10.1021/ja202739j |J. Am. Chem. Soc. 2011, 133, 10587–10598

Table 5. Experimental and Predicted ^{29}Si NMR Chemical Shifts of Ordered Na-GaNAT-III(A), K-GaNAT-III(E), and K-GaNAT-III(EC) Materials

			^{29}Si δ, ppm from TMS											
			Na-GaNAT-III(A)				K-GaNAT-III(E)				K-GaNAT-III(EC)			
Si site	multiplicity	structural unit	∠T−O−T[a]	δ_{pre}[b]	δ_{obs}[c]	Δδ[d]	∠T−O−T[a]	δ_{pre}[b]	δ_{obs}[c]	Δδ[d]	∠T−O−T[a]	δ_{pre}[b]	δ_{obs}[c]	Δδ[d]
T1	8	Si_1(4Ga)	141.7	−79.4	−80.2 [4.4]	0.2	137.2	−77.3			135.6	−76.5	−76.2 [15.2]	0.3
		Si_1(3Ga)		−86.1	−85.3 [1.9]	0.8		−84.0				−83.2	−86.0 [24.6]	2.8
		Si_1(2Ga)		−92.8	−94.8 [31.1]	−2.0		−90.7	−90.6 [31.7]	0.1		−89.9		
		Si_1(1Ga)		−99.5				−97.4				−96.6		
		Si_1(0Ga)		−106.2				−104.1				−103.3		
T2	16	Si_2(4Ga)	134.6	−76.0	−76.5 [1.1]	−0.5	134.5	−75.9			130.5	−73.6		
		Si_2(3Ga)		−82.7	−84.6 [61.6]	−1.9		−82.6	−84.1 [65.9]	−1.5		−80.3	−77.3 [51.1]	3.0
		Si_2(2Ga)		−89.4				−89.3	−89.6 [2.4]	−0.3		−87.0	−86.6 [9.0]	0.2
		Si_2(1Ga)		−96.1				−96.0				−93.7		
		Si_2(0Ga)		−102.8				−102.7				−100.4		
		Si/Ga_{NMR}		$Si/Ga_{NMR,Fdd2}$ = 1.46				$Si/Ga_{NMR,Fdd2}$ = 1.50				$Si/Ga_{NMR,Fdd2}$ = 1.31		

[a] Average T−O−T angles in degrees from the crystallographic data obtained in this work. [b] Predicted chemical shifts from the average T−O−T angles using the equation of Cho et al.[7a] [c] Observed chemical shifts (from the deconvolution of the experimental spectra) with their relative intensities given in square brackets. [d] $\Delta\delta = \delta_{obs} - \delta_{pre}$, the difference between observed and predicted chemical shifts.

Table 6. Experimental and Predicted ^{29}Si NMR Chemical Shifts of Disordered Na-GaNAT-I(A), K-GaNAT-I(E), and K-GaNAT-I(EC) Materials

			^{29}Si δ, ppm from TMS											
			Na-GaNAT-I(A)				K-GaNAT-I(E)				K-GaNAT-I(EC)			
Si site	multiplicity	structural unit	∠T−O−T[a]	δ_{pre}[b]	δ_{obs}[c]	Δδ[d]	∠T−O−T[a]	δ_{pre}[b]	δ_{obs}[c]	Δδ[d]	∠T−O−T[a]	δ_{pre}[b]	δ_{obs}[c]	Δδ[d]
T1	8	Si_1(4Ga)	138.4	−77.9	−79.6 [3.1]	−1.7	133.8	−75.5	−77.1 [2.0]	−1.6	135.4	−76.4	−77.2 [6.8]	−0.8
		Si_1(3Ga)		−84.6	−85.1 [4.5]	−0.5		−82.2	−83.5 [9.9]	−1.3		−83.1	−84.7 [9.1]	−1.6
		Si_1(2Ga)		−91.3	−91.3 [9.7]	0.0		−88.9	−89.6 [6.6]	−0.7		−89.8		
		Si_1(1Ga)		−98.0	−98.6 [8.8]	−0.6		−95.6	−97.1 [1.6]	−1.5		−96.5		
		Si_1(0Ga)		−104.7	−106.5 [0.8]	−1.8		−102.3				−103.2		
T2	16	Si_2(4Ga)	134.5	−75.9	−78.5 [6.5]	−2.6	134.5	−75.9	−77.1 [4.0]	−1.2	131.4	−74.1	−71.5 [22.3]	2.6
		Si_2(3Ga)		−82.6	−83.8 [14.2]	−1.2		−82.6	−83.5 [19.7]	−0.9		−80.8	−79.7 [19.4]	1.1
		Si_2(2Ga)		−89.3	−88.2 [8.9]	1.1		−89.3	−89.6 [13.2]	−0.3		−87.5		
		Si_2(1Ga)		−96.0	−94.3 [5.5]	1.7		−96.0	−97.1 [3.2]	−1.1		−94.2		
		Si_2(0Ga)		−102.7	−101.4 [1.4]	1.3		−102.6				−100.9		
T3	16	Si_3(4Ga)	134.4	−75.9	−78.5 [6.5]	−2.6	134.8	−76.1	−77.1 [4.0]	−1.0	132.5	−74.8	−75.6 [17.6]	−0.8
		Si_3(3Ga)		−82.6	−83.8 [14.2]	−1.2		−82.8	−83.5 [19.7]	−0.7		−81.5	−83.5 [8.4]	−2.0
		Si_3(2Ga)		−89.3	−88.2 [8.9]	1.1		−89.5	−89.6 [13.2]	−0.1		−88.2	−89.4 [16.3]	−1.2
		Si_3(1Ga)		−96.0	−94.3 [5.5]	1.7		−96.2	−97.1 [3.2]	−0.9		−94.9		
		Si_3(0Ga)		−102.7	−101.4 [1.4]	1.3		−102.9				−101.6		
		Si/Ga_{NMR}		$Si/Ga_{NMR,Fdd2}$ = 1.69				$Si/Ga_{NMR,Fdd2}$ = 1.68				$Si/Ga_{NMR,Fdd2}$ = 1.23		

[a] Average T−O−T angles in degrees from the crystallographic data obtained in this work. [b] Predicted chemical shifts from the average T−O−T angles using the equation of Cho et al.[7a] [c] Observed chemical shifts (from the deconvolution of the experimental spectra) with their relative intensities given in square brackets. [d] $\Delta\delta = \delta_{obs} - \delta_{pre}$, difference between observed and predicted chemical shifts.

angles apparently forces several ^{29}Si resonances to overlap, and we have actually been able to find a deconvolution that agrees well with the refined structure, with disagreements smaller than 2 ppm and a calculated Si/Ga ratio of 1.68, essentially identical to the value (1.65) determined by elemental analysis (Table 5). Given the decreased number of distinct resonances, the spectrum would leave open the possibility that the exchange process could have promoted a large degree of T-atom ordering. However, this possibility may be ruled out by analyzing the upper two spectra in Figure 5. The ^{29}Si MAS NMR spectrum of the dehydrated K-GaNAT-I(EC) material highly resembles that of the parent Na-GaNAT-I(A) material, with a similar overall distribution of intensities and no less than 7 resonances visible to the naked eye, but shifted by ca. 8 ppm to lower field. We should note here that the refined crystal structure of K-GaNAT-I(EC) again shows a range of average T−O−T angles similarly broad as that of Na-GaNAT-I(A), although more acute (135.4°, 131.4°, and 132.5° for T1, T2, and T3, respectively). More conclusively, back-exchange to its Na^+ form is possible in this case, and the corresponding spectrum may be almost exactly superimposed to that of Na-GaNAT-I(A). This confirms that the initial K^+ ion exchange and the subsequent calcination steps do not modify the T-atom ordering in any significant extent.

DISCUSSION

As described above, sodium gallosilicate natrolites with the same framework composition are selective for monovalent

Table 7. Thermodynamic Cycle to Calculate the K^+ Ion Exchange Enthalpy of Sodium Gallosilicate Natrolite Zeolites[a]

$Na_xGa_xSi_{1-x}O_2 \bullet mH_2O$ (s, 25 °C) → xNa^+ (700 °C, soln) + xGa^{3+} (700 °C, soln) + $Si_{1-x}^{4+}O_2$ (700 °C, soln) + mH_2O (700 °C, g)	ΔH_1
$K_xGa_xSi_{1-x}O_2 \bullet nH_2O$ (*s*, 25 °C) → xK^+ (700 °C, soln) + xGa^{3+} (700 °C, soln) + $Si_{1-x}^{4+}O_2$ (700 °C, soln) + nH_2O (700 °C, g)	ΔH_2
xNa^+ (700 °C, soln) → xNa^+ (25 °C, soln)	ΔH_3
xK^+ (700 °C, soln) → xK^+ (25 °C, soln)	ΔH_4
$(m-n)H_2O$ (700 °C, g) → $(m-n)H_2O$ (25 °C, l)	$\Delta H_5 = -68.9(m-n)$ kJ mol^{-1}
$Na_xGa_xSi_{1-x}O_2 \bullet mH_2O$ (s, 60 °C) + xK^+ (soln, 60 °C) → $K_xGa_xSi_{1-x}O_2 \bullet nH_2O$ (s, 60 °C) + xNa^+ (soln, 60 °C) + $(m-n)H_2O$ (60 °C, *l*)	ΔH_6
ΔH_6[b] = $\Delta H_1 - \Delta H_2 + \Delta H_3 - \Delta H_4 + \Delta H_5 \sim \Delta H_1 - \Delta H_2 + \Delta H_5$	

[a] ΔH_1 and ΔH_2 are drop solution enthalpies (ΔH_{DS}) per mole of TO_2 (*T* = Si or Ga) of the Na^+ and K^+ forms of gallosilicate zeolites, respectively. ΔH_3 and ΔH_4 are heat contents of Na^+ and K^+ from 700 to 25 °C, respectively. [b] ΔH_3 and ΔH_4 are likely small enough to be ignored (see the text).

Table 8. K^+ Ion Exchange Enthalpies per Mole of TO_2 of Sodium Gallosilicate Natrolites

material	$\Delta H_{DS,Na}$, kJ mol^{-1}	$\Delta H_{DS,K}$, kJ mol^{-1}	$\Delta H_{DS,Na} - \Delta H_{DS,K}$	$(H_2O/TO_2)_{Na}$	$(H_2O/TO_2)_K$	$\Delta(H_2O/TO_2)$	ΔH_{KIE}[a]
Na-GaNAT(I)	107.6 ± 0.9	109.9 ± 0.9	−2.3	0.488	0.510	−0.023	−0.7
Na-GaNAT(II)	108.2 ± 2.3	108.8 ± 0.7	−0.6	0.433	0.470	−0.038	2.0
Na-GaNAT(III)	107.9 ± 0.7	103.9 ± 0.6	4.0	0.400	0.405	−0.005	4.3

[a] K^+ ion exchange enthalpy (kJ mol^{-1} of TO_2) defined by $\Delta H_{DS,Na} - \Delta H_{DS,K} - 68.9\Delta(H_2O/TO_2)$, where $\Delta(H_2O/TO_2)$ is $(H_2O/TO_2)_{Na} - (H_2O/TO_2)_K$.

cations, and their cation exchange performance depends on the degree of Si−Ga ordering and on the size of the cation to be exchanged into the zeolite. On the basis of the different stabilities of the different materials involved, we may postulate that the better cation exchange performance of the as-made sodium materials upon decreasing the degree of ordering is due to the lower stability, relative to the exchanged zeolite, of the more disordered material. The degree of exchange depends on the thermodynamics of the reaction

$$\text{Na-NAT(s)} + M^+(\text{soln}) \leftrightarrow \text{M-NAT(s)} + Na^+(\text{soln}) \quad (1)$$

with $\Delta G°$ determining the equilibrium constant through $\Delta G° = -RT \ln K$ and $K = [Na^+]/[K^+]$.

A recent report on the energetics of the sodium and potassium gallosilicate natrolites affords an estimate of not $\Delta G°$ but $\Delta H°$ of the K^+/Na^+ exchange at 25 °C (not 60 °C as in the actual reaction, but the difference cannot be large).[22] On the basis of the thermodynamic cycle summarized in Table 7 and on the data in ref 22, we have estimated the ΔH values listed in Table 8. In the calculation we have assumed that the heat contents of Na^+ and K^+ from 700 to 25 °C are small enough to be neglected. Also, we contend that, even if they are not that small, their contribution must be quite similar in the three reactions, given the similar cation contents of the three starting sodium materials. Hence, the values in Table 8 could provide a good qualitative estimation of the relative energetics of the ion exchange reaction. Indeed, the values obtained suggest that the exchange reaction is thermodynamically more favorable when the degree of T-atom ordering decreases, although the differences are certainly small and the lack of thermodynamic data on the other cation-exchanged natrolites limits the extent of this conclusion. Additionally, the speculation that the different cation exchange abilities of the three natrolites are purely thermodynamic may be challenged by two points: first, the conditions of the exchange reaction (large excess of the exchanging cation and repeated experiments) would favor complete exchange because of Le Chatelier's principle. This is the case for the back-exchange of potassium natrolites to their Na^+ form, which is easily achieved for the three materials, while the thermodynamic data in Table 8 suggest rather small thermodynamic hindrance for Na-GaNAT-I compared to the more ordered material. Second and most importantly, the crystallographic data suggest that in most cases the exchange may suffer from severe steric hindrance. Hence, kinetics may be of more importance than thermodynamics in the overall processes.

The ease of Na^+ back-exchange of all the hydrated potassium materials can be understood by their relatively large pore sizes. For all the other materials (parent Na-GaNAT, dehydrated K-GaNAT, and hydrated or dehydrated Rb-GaNAT-I materials); however, the small pore sizes compared to that of the intervening cations suggest that, from a kinetic point of view, cation exchange would be much hindered, unless the zeolite framework is able to dynamically deform, to a large extent. The pore window must significantly expand its size during the exchange process in order to allow the passage of Na^+ (or Rb^+ and K^+ in the back-exchange experiments) out and the larger K^+, Rb^+ in (and even Cs^+ in the case of Na-GaNAT-I). Such a deformation cannot be limited to the pore mouth, because full cation exchange is achieved, for example, with K^+ and Rb^+ for this disordered material. In other words, the deformation cannot be an effect limited to the outer surface, but involves the traffic of cations through the bulk material, implying a large flexibility of the NAT framework. If the framework flexibility is really needed for cation exchange, the different cation exchange results in Table 2 lead us to hypothesize that the magnitude of the required dynamic deformation in natrolites decreases as the degree of Si−Ga ordering increases. In the following we would like to rationalize this hypothesis and to reflect on the flexibility in zeolites and its plausible dependence on T-atom ordering when Si is substituted by a larger and much more electropositive element.

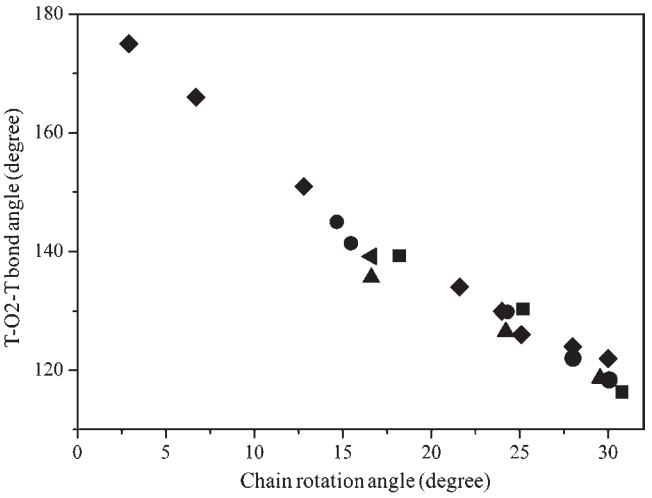

Figure 6. T−O2−T bond angles of GaNAT-I (circle), GaNAT-II (triangle), GaNAT-III (square) materials with different extraframework compositions vs their natrolite chain rotation angles. Angles of various cation forms (diamond) of a natural aluminosilicate natrolite from ref 21, together with the angle of K-PST-1 (tilted triangle) from ref 18, are also included for comparison.

Flexibility in zeolites may be discussed as a property inherent to their framework topology, which is generally considered as built from quite stiff tetrahedra joined through rather floppy O linkages.[23] In fact, there are several studies concerning the flexibility of different zeolite topologies with the same composition.[24] Here we will refer to this concept with the term "topological flexibility". However, it has also been shown that T-atom substitutions may alter the flexibility of a given zeolite framework: elements more electropositive than Si induce an increase in the ionicity of the TO_4 tetrahedra, yielding them less stiff and more deformable ("substitution-induced flexibility").[5,25] Here we want to reflect on the plausible effect of T-atom ordering on the flexibility of zeolites that belong to the same framework type and have similar chemical compositions.

The topological flexibility of aluminosilicate natrolite minerals has long been noticed.[20] In fact, this family of zeolites has been classified among the "fibrous" zeolites, in which the framework is said to be more rigid along the *c*-axis than along the other two axes.[26] The crystal structure of natrolite was proposed by Pauling more than 80 years ago,[20a] when he pointed out that the structure is made of rigid and noncompressible "strings", the so-called natrolite chain, that are assembled into a structure that, as a whole, is flexible: it collapses by rotating the natrolite chains around their axes in order to attain minimum interatomic distances. Other studies supported this notion,[20,21] and it has been noticed in aluminosilicate natrolites that the unit cell volume may change much, but the change is larger on the *a*- and *b*-axes than on the *c*-axis (i.e., the natrolite chain is rather rigid within itself, but a lot of framework flexibility is allowed by rotating the chain through the O hinges that connect them). Walton, Evans, and co-workers also have showed an anisotropic behavior consistent with this model in their studies on the mechanical properties of natrolites.[27] In a recent report on the selective adsorption of small gases by PST-1, a potassium gallosilicate natrolite with a very low degree ($S = 0.10$) of Si−Ga ordering, we have already pointed out that the experimental results should be understood by considering the high flexibility of the framework. This was substantiated by the observed large unit cell shrinkage (ca. 16%) of the material upon reversible dehydration, with no noticeable structural degradation.[18] Natural aluminosilicate natrolites displaying full Si−Al ordering have been reported to shrink around 18 or 24% upon dehydration to the so-called metanatrolite phase,[20c,d] although in this case substantial structural degradation does occur. Finally, natural aluminosilicate minerals with the NAT topology (e.g., natrolite, scolecite, and mesolite), as well as a synthetic potassium gallosilicate natrolite (Si/Ga = 1.5), undergo a significant expansion of their cells by "superhydration" induced under hydrostatic (alcohol/water) pressures of 0.8−1.5 GPa.[28]

As commented above, the topological flexibility of natrolites relies on the concerted rotation, clockwise and counterclockwise, of adjacent natrolite chains along their axis.[20] The fully expanded structure with more circular pores corresponds to no chain rotation, while the larger the rotation (up to 45°), the more elliptical and narrower become the channels. Alberti and Vezzalini[20d] already showed that the rotation angle ψ[29] (defined as the mean of the angles between the sides of the quadrilateral around the chain with the *a*- or *b*-axis) is rather independent of the degree of T-atom ordering in sodium aluminosilicate natrolites (where ψ is in the 20°−24° range). The overall results of our study confirm that this conclusion is also applicable to gallosilicate natrolites: ψ is rather independent of the degree of ordering but depends much on the nature of the cation and hydration state. For our as-made sodium gallosilicate materials, ψ is in the range 24.2°−25.2°, and their pores are much similar in size and shape to one another.

The rotation of chains hinges on the oxygen atom O2, which joins one Si tetrahedra with one Ga tetrahedra for the totally ordered material. As seen in Figure 6, in fact, there is a good correlation between the angle of rotation of the chains, ψ, and the T−O2−T angle, θ, not only for the 11 crystal structures presented in this work, but also for K-PST-1, a highly disordered NAT material with a high Ga content, and fully ordered natural aluminosilicates and their various cation-exchanged forms,[18,21] all the synchrotron diffraction data of which have been successfully indexed as orthorhombic, space group *Fdd*2, regardless of their framework and extraframework compositions. Furthermore, and very interestingly, there is also a good correlation between the unit cell volume and any of their θ or ψ angles (Figure 7). Strikingly, there appear to be two different slopes in the correlations shown in Figure 7, one for small volumes and another and steeper one for larger volumes. This implies that beyond some point any further expansion of the framework implies a larger change in the angles. The correlations in Figures 6 and 7 are highly independent of chemical composition (nature and amount of countercations, nature and amount of heteroatoms) and degree of T-atom ordering, so they nicely illustrate the concept of topological flexibility commented above.

In addition to the rotation of natrolite chains pointed out by Pauling, however, the chains themselves can undergo a twist that reduces the *c* unit cell edge in aluminosilicate metanatrolite (dehydrated natrolite).[20d] Also, Baur and co-workers studied the Li^+ form of a natural fully ordered natrolite prepared by a melted salt process and found that the material has a shortened *c*-axis due to a twist within the natrolite chain itself.[29] Besides the traditional, topological view of flexibility in natrolite zeolites by rotation of rigid chains, therefore, we should consider the possibility of twists of the chain. When the unit cell parameters (Supporting Information Tables S1−S3) of gallosilicate

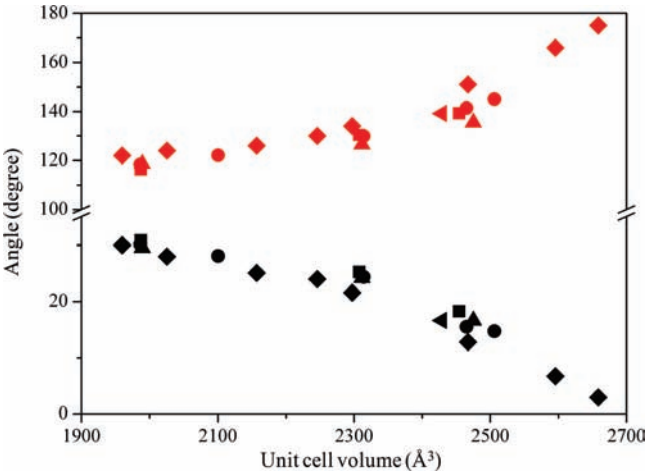

Figure 7. T−O2−T bond angles (red) and natrolite chain rotation angles (blue) of GaNAT-I (circle), GaNAT-II (triangle), GaNAT-III (square) materials with different extraframework compositions vs their unit cell volumes. Included for comparison are angles of various cation forms (diamond) of a natural aluminosilicate natrolite from ref 21, as well as the angle of K-PST-1 (tilted triangle) from ref 18.

materials with the same countercation (Na^+, K^+, or Rb^+) and same hydration state (hydrated or dehydrated) are compared, in fact, we can see that the orthorhombic distortion increases upon increasing the degree of T-atom ordering, as previously reported.[3,7] As can be seen in Supporting Information Figure S6, in addition, the unit cell parameter *c* decreases. This decrease in *c* unit cell edge is due to the increased replacement of Ga by the smaller Si at T1, i.e., at the only T-site that is only bonded to tetrahedra in the same natrolite chain and, thus, shall be accompanied by an increase in the rigidity of the natrolite chain because of the higher covalent character of the Si−O bond compared to the Ga−O bond.

The cation exchange results shown in Tables 2 and 3 suggest that while there is a sieving effect, the zeolite pores need to deform to allow the cation exchange. Given that the sieving effect depends on the degree of Si−Ga ordering, we propose that deformation might also depend on the degree of ordering. In other words, cation exchange in natrolite zeolites is mediated by their framework flexibility, but the flexibility would decrease as the degree of ordering increases, giving rise to a T-atom ordering dependent sieving effect. The substitution in T-sites of Si by the larger and more electropositive Ga should increase the flexibility within the tetrahedra, and hence the framework flexibility, because the T−O bond becomes more ionic and, hence, the bonds are less spatially oriented.[5,25] Since the Si/Ga ratio in our three gallosilicate natrolites with different degrees of ordering is essentially the same, the overall ionicity and overall "substitution-induced flexibility" would also be expected to be similar. Actually, Na-GaNAT-II and Na-GaNAT-III have a slightly higher Ga content than Na-GaNAT-I. Thus, they would be expected to be slightly more flexible. However, the cation exchange results would suggest otherwise, so it might be concluded that, if flexibility indeed plays a role, Ga siting in different tetrahedra may have a significant impact on the pore deformation needed for exchange. If cation exchange would rely on the chain rotation only, one would expect the most ordered Na-GaNAT-III material to be a better cation exchanger due to a greater flexibility of the Si−O2−Ga bond. By contrast, partial siting of Ga on T1, i.e., on the unique tetrahedrum that is connected only to tetrahedra of the same natrolite chain, by increasing the ionicity of the $(T1)O_4$ tetrahedra would afford compression and expansion of the chain itself, which provides a second mechanism for flexibility that might dynamically expand the pore. This hypothesis may explain the results in Tables 2 and 3, since the higher the degree of disorder, the larger the Ga population in T1.

CONCLUSIONS

The cation exchange ability of sodium gallosilicate natrolites strongly depends on their degree of Si−Ga ordering. The thermodynamics of the Na^+/K^+ exchange would suggest only a small preference for exchange in the most disordered zeolite. However, the size of the pores of all of the as-made materials is close to that of the bare Na^+ cation, implying the need for an extensive framework deformation that dynamically changes the pore size. While Na^+ back-exchange of hydrated K^+-exchanged natrolites occurs readily, on the other hand, that of dehydrated potassium materials, whose pore sizes are significantly smaller, again shows a strong dependency on T-atom ordering. We propose as a hypothesis that the framework flexibility of these natrolites, which is always large, is enhanced by siting of a fraction of Ga on the lower multiplicity site T1. This site belongs completely to the natrolite chain, in the sense that it is only bonded to T-sites within the same chain, so substitution of Si by the larger and more electropositive Ga would increase the ionicity of the T-O bond, thus enhancing the flexibility of the chain itself. Another important influence of ordering on the physicochemical properties of these zeolites is revealed after calcination of the K^+-exchanged forms: the most ordered material becomes non-microporous, as it is unable not only to back-exchange but also rehydrate or adsorb small molecules such as He or H_2. The materials studied here are channel-based, small-pore zeolites with a poor thermal stability, especially in the case of the acid form,[7a] which makes it very difficult, or even impossible, to precisely examine the effects of the degree of T-atom ordering on their other important properties, such as catalytic and adsorption properties. Given the overall results of our study, however, it is clear that T-atom ordering in zeolite frameworks is a key factor affecting the physicochemical properties of this unique class of microporous solids.

ASSOCIATED CONTENT

Supporting Information. Additional information as noted in the text (PDF). This material is available free of charge via the Internet at http://pubs.acs.org.

AUTHOR INFORMATION

Corresponding Author
sbhong@postech.ac.kr

ACKNOWLEDGMENT

Financial support for this work was provided by the National Research Foundation of Korea (R0A-2007-000-20050-0 and 2009-0092793) and by the Carbon Dioxide Reduction and Sequestration R&D Center (16-2008-02-005-01). M.A.C. also gratefully acknowledges additional funding by the Spanish CICYT (project MAT2009-09960). The work at Pohang Acceleration Laboratory (PAL) was supported in part by the Ministry

of Science and Technology of Korea and POSTECH. We thank the staffs at 8C2, PAL, for their assistance with the powder diffraction measurements and Prof. C.M. Zicovich-Wilson (UA Estado de Morelos) and Dr. W. Zhou (UC Davis) for helpful discussions and suggestions.

REFERENCES

(1) (a) Newsam, J. M. *Science* **1986**, *231*, 1093–1099. (b) Sherman, J. D. *Proc. Natl. Acad. Sci. U. S. A.* **1999**, *96*, 3471–3478. (c) Tsapatsis, M. *AIChE J.* **2002**, *48*, 654–660.

(2) Camblor, M. A.; Hong, S. B. In *Porous Materials*; Bruce, D. W., O'Hare, D., Walton, R. I., Eds.; Wiley: Chichester, 2011; pp 265−325.

(3) Camblor, M. A.; Corma, A.; Valencia, S. *Microporous Mesoporous Mater.* **1998**, *25*, 59–74.

(4) Souverijns, W.; Rombouts, L.; Martens, J. A.; Jacobs, P. A. *Microporous Mater.* **1995**, *4*, 123–130.

(5) Hong, S. B.; Lee, S.-H.; Shin, C.-H.; Woo, A. J.; Alvarez, L. J.; Zicovich-Wilson, C. M.; Camblor, M. A. *J. Am. Chem. Soc.* **2004**, *126*, 13742–13751.

(6) Loewenstein, W. *Am. Mineral.* **1954**, *39*, 92–96.

(7) (a) Cho, H. H.; Kim, S. H.; Kim, Y. G.; Kim, Y. C.; Koller, H.; Camblor, M. A.; Hong, S. B. *Chem. Mater.* **2000**, *12*, 2292–2300. (b) Paik, W. C.; Camblor, M. A.; Hong, S. B. *Stud. Surf. Sci. Catal.* **2001**, *135*, 05-P-07 (CD-ROM).

(8) Altomare, A.; Camalli, M.; Cuocci, C.; Giacovovazzo, C.; Moliterni, A.; Rizzi, R. *J. Appl. Crystallogr.* **2009**, *42*, 1197–1202.

(9) (a) Rietveld, H. M. *J. Appl. Crystallogr.* **1969**, *2*, 65–71. (b) Larson, A.; von Dreele, R. B. *General Structure Analysis System GSAS*; Los Alamos National Laboratory: Los Alamos, NM, 2000. (c) Toby, B. H. *J. Appl. Crystallogr.* **2001**, *34*, 210–213.

(10) Hastings, J. B.; Thomlinson, W.; Cox, D. E. *J. Appl. Crystallogr.* **1984**, *17*, 85–95.

(11) Baerlocher, Ch.; McCusker, L. B. Database of Zeolite Structures, http://www.iza-structure.org/databases/.

(12) Alberti, A.; Cruciani, G.; Dauru, I. *Eur. J. Mineral.* **1995**, *7*, 501–508.

(13) Sherry, H. S. In *Handbook of Zeolite Science and Technology*; Auerbach, S. M., Carrado, K. A., Dutta, P. K., Eds.; Marcel Dekker: New York, 2003; pp 1007−1062.

(14) Barrer, R. M. *J. Chem. Soc.* **1950**, 2342–2350.

(15) (a) Taylor, W. H.; Meek, C. A.; Jackson, W. W. *Z. Kristallogr.* **1933**, *84*, 373–398. (b) Fälth, L.; Hansen, S. *Acta Crystallogr.* **1979**, *B35*, 1877–1880. (c) Stuckenschmidt, E.; Joswig, W.; Baur, W. H.; Hofmeister *Phys. Chem. Mineral.* **1997**, *24*, 403–410.

(16) Cotton, F. A.; Wilkinson, G.; Murillo, C. A.; Bochmann, M. *Advanced Inorganic Chemistry*, 6th ed.; Wiley: New York, 1999.

(17) Breck, D. W. *Zeolite Molecular Sieves*; Wiley: New York, 1974; p 636.

(18) (a) Shin, J.; Camblor, M. A.; Woo, H. C.; Miller, S. R.; Wright, P. A.; Hong, S. B. *Angew. Chem., Int. Ed.* **2009**, *48*, 6647–6649. (b) Shin, J.; Kim, S. H.; Camblor, M. A.; Warrender, S. J.; Miller, S. R.; Zhou, W.; Wright, P. A.; Hong, S. B. *Dalton Trans.* **2010**, *39*, 2246–2253.

(19) Shannon, R. D. *Acta Crystallogr.* **1976**, *A32*, 751–797.

(20) (a) Pauling, L. *Proc. Natl. Acad. Sci. U. S. A.* **1930**, *16*, 453–459. (b) Taylor, W. H. *Proc. R. Soc. London A* **1934**, *145*, 80–103. (c) Fang, J. H. *Am. Mineral.* **1963**, *48*, 414–417. (d) Alberti, A.; Vezzalini, G. *Neues Jb. Miner. Monat.* **1983**, 135–144. (e) Wang, H. W.; Bish, D. L. *Am. Mineral.* **2008**, *93*, 1191–1194.

(21) (a) Lee, Y.; Lee, Y.; Seoung, D. *Am. Mineral.* **2010**, *95*, 1636–1641. (b) Lee, Y.; Seoung, D.; Liu, D.; Park, M. B.; Hong, S. B.; Chen, H.; Bai, J.; Kao, C.-C.; Vogt, T.; Lee, Y. *Am. Mineral.* **2011**, *96*, 393–401.

(22) Zhou, W.; Navrotsky, A.; Shin, J.; Hong, S. B. *Microporous Mesoporous Mater.* **2010**, *135*, 197–200.

(23) Hammonds, K. D.; Heine, V.; Dove, M. T. *J. Phys. Chem. B* **1998**, *102*, 1759–1767.

(24) Sartbaeva, A.; Wells, S. A.; Treacy, M. M. J.; Thorpe, M. F. *Nat. Mater.* **2006**, *5*, 962–965.

(25) Blasco, T.; Corma, A.; Dıaz-Cabanas, M. J.; Rey, F.; Vidal-Moya, J. A.; Zicovich-Wilson, C. M. *J. Phys. Chem. B* **2002**, *106*, 2634–2642.

(26) Barrer, R. M. *Discuss. Faraday Soc.* **1949**, *7*, 135–141.

(27) (a) Lethbridge, Z. A. D.; Williams, J. J.; Walton, R. I.; Smith, C. W.; Hooper, R. M.; Evans, K. E. *Acta Mater.* **2006**, *54*, 2533–2545. (b) Williams, J. J.; Smith, C. W.; Evans, K. E.; Lethbridge, Z. A. D.; Walton, R. I. *Chem. Mater.* **2007**, *19*, 2423–2434.

(28) (a) Lee, Y.; Vogt, T.; Hriljac, J. A.; Parise, J. B.; Artioli, G. *J. Am. Chem. Soc.* **2002**, *124*, 5466–5475. (b) Lee, Y.; Vogt, T.; Hriljac, J. A.; Parise, J. B.; Hanson, J. C.; Kim, S. J. *Nature* **2002**, *420*, 485–489.

(29) Baur, W. H.; Kassner, D; Kim, C.-H.; Sieber, N. H. *Eur. J. Mineral.* **1990**, *2*, 761–769.